SLEEPJ, 2020, 1–14

doi: 10.1093/sleep/zsaa085
Advance Access Publication Date: 28 April 2020
Original Article

ORIGINAL ARTICLE

Gene expression analysis in the mouse brainstem identifies Cart and Nesfatin as neuropeptides coexpressed in the Calbindin-positive neurons of the *Nucleus papilio*

Franck Girard[1,*], Michelle von Siebenthal[1], Fred P. Davis[2,3] and Marco R. Celio[1]

[1]Department of Medicine, Faculty of Science, University of Fribourg, Fribourg, Switzerland, [2]Janelia-Farm Research Campus, Howard Hughes Medical Institute, Ashburn, VA and [3]Present address: Molecular Immunology and Inflammation Branch, National Institute of Arthritis and Musculoskeletal and Skin Diseases, National Institute of Health, Bethesda, MA.

*Corresponding author. Franck Girard, Anatomy and Program in Neuroscience, Department of Medicine, Faculty of Science, University of Fribourg, Route A. Gockel 1, CH1700 Fribourg, Switzerland. Email: franck.girard@unifr.ch.

Abstract

Study Objectives: The brainstem contains several neuronal populations, heterogeneous in terms of neurotransmitter/neuropeptide content, which are important for controlling various aspects of the rapid eye movement (REM) phase of sleep. Among these populations are the Calbindin (Calb)-immunoreactive NP^{Calb} neurons, located in the *Nucleus papilio*, within the dorsal paragigantocellular nucleus (DPGi), and recently shown to control eye movement during the REM phase of sleep.
Methods: We performed in-depth data mining of the in situ hybridization data collected at the Allen Brain Atlas, in order to identify potentially interesting genes expressed in this brainstem nucleus. Our attention focused on genes encoding neuropeptides, including Cart (Cocaine and Amphetamine Regulated Transcripts) and Nesfatin 1.
Results: While nesfatin 1 appeared ubiquitously expressed in this Calb-positive neuronal population, Cart was coexpressed in only a subset of these glutamatergic NP^{Calb} neurons. Furthermore, an REM sleep deprivation and rebound assay performed with mice revealed that the Cart-positive neuronal population within the DPGi was activated during REM sleep (as measured by c-fos immunoreactivity), suggesting a role of this neuropeptide in regulating some aspects of REM sleep.
Conclusions: The assembled information could afford functional clues to investigators, conducive to further experimental pursuits.

Statement of Significance

Several physiological and behavioral features are characteristics of the rapid eye movement (REM) phase of sleep, also called paradoxical sleep. These include muscle atonia, desynchronized EEG activity, vivid dreaming, and rapid eye movements. A small cluster of Calbindin-immunoreactive neurons (namely, the *Nucleus papilio*) has been recently identified in the brainstem and shown to be both necessary and sufficient for triggering eye movement during REM sleep. In the present study, we performed data mining of the in situ hybridization data collected at the Allen Brain Atlas, in order to identify genes expressed in these neurons. Our data show that the neuropeptide Cart (Cocaine and Amphetamine Regulated Transcript) is expressed in some of these Calbindin-immunoreactive neurons and that these Cart-neurons are activated during REM sleep.

Key words: *Nucleus papilio*; NPCalb; REM sleep; DPGi; calbindin; Cart; nesfatin

Submitted: 11 December, 2019; **Revised:** 8 April, 2020

Introduction

Several physiological and behavioral features are characteristics of the REM phase of sleep, also called paradoxical sleep. These include rapid eye movements, vivid dreaming, desynchronized electroencephalogram activity, and atonia of the postural muscles [1]. Among several brainstem structures that have been shown to be involved during REM sleep [2–6], the dorsal paragigantocellular nucleus (DPGi) appears as a very crucial area in sleep regulation, as it contains neurons of different nature, which apparently play particular roles in regulating some aspects of REM sleep. Indeed, GABAergic neurons of the DPGi were proposed to inhibit the noradrenergic wake-promoting neurons of the *Locus ceruleus*, the dorsal raphé nucleus, and the ventrolateral periaqueductal gray, thereby favoring the initiation of REM sleep [4, 7, 8]. Within the DPGi we recently identified the *Nucleus papilio* (NP^{Calb}) as a bilateral, symmetric cluster of glutamatergic neurons expressing the calcium-binding protein Calbindin-D28k (Calb) [9]. Calb immunoreactivity in this nucleus is conserved in rodents (mouse and rat), monkey, and human. In mouse, it densely projects to the three contralateral eye-muscle nuclei (abducens, trochlear, and oculomotor), but also to several brain areas contributing to REM sleep control including the MCH-neurons of the lateral hypothalamus, the subcoeruleus nucleus (SubC), the pontine reticular formation (PnC), and the gigantocellular reticular nucleus (Gi). Noteworthy, activating or inactivating these neurons by means of optogenetics demonstrated both the necessity and sufficiency of the NP^{Calb} for triggering eye movement during REM sleep [9].

The automated ALLENMINER search [10] of in situ hybridization (ISH) images in the Allen Brain Atlas (ABA) can be implemented to identify genes that are expressed in rather small agglomerations of cells, such as the PV1/Parvafox nucleus (parvalbumin-FoxB1 immunoreactive nucleus) in the lateral hypothalamus [11]. Using this protocol, potentially interesting information respecting very small neuronal populations can be elicited. By this means, ISH on adjacent sections has hitherto revealed most of the genes that were tested to be coexpressed with the mRNA for *Pvalb* [11]. We were therefore sanguine that a similar search would facilitate molecular and potentially functional characterization of the Calb-expressing neurons of the NP^{Calb}. In addition, we screened the AGEA (Anatomic Gene expression Atlas) [12] at the ABA, focusing on genes expressed in the NP^{Calb}/DPGi area.

Methods

Animals

For analyzing the expression of several proteins potentially coexpressed in the NP^{Calb}, 15 C57BL/6J mice (from our animal facility) of both sexes, aged 10–14 weeks, as well as 3 Wistar rats (Janvier, Lyon, France), were used. For the analysis of the neurotransmitter status of the Cart-expressing neurons, two mice of each genotype were used (*Slc17a6*::Cre and *Slc32a1*::Cre encoding, respectively, VGlut2 glutamate and VGat GABA transporters, both obtained from the Jackson Laboratory; *Slc6a5*-GFP::Cre mice encoding the Glyt2 glycine transporter, obtained from Dr Zeilhofer, Pharmacology, Zurich). Fifteen C57BL/6J female mice were included in the REM sleep deprivation and rebound assay.

All animals were housed in our animal facilities and in accordance with the relevant Swiss laws. The Veterinary Commission for Animal Research of the Canton of Fribourg (Switzerland) approved this study.

Animals were anesthetized with pentobarbital (100 mg/kg of body weight) and then perfused via the left ventricle, first with chilled (4°C) physiological (0.9%) saline and then with chilled (4°C) 4% paraformaldehyde. The brains were excised and post-fixed overnight at 4°C in 4% paraformaldehyde and subsequently immersed in 0.1 M Tris buffer (pH 7.3) containing 20% sucrose in preparation for cryo-sectioning.

Immunohistochemistry

The various brain specimens were cryo-sectioned into 30, or 40, µm coronal sections and collected directly in 0.1 M Tris buffer containing 0.02% sodium azide, within which they were maintained until the time of analysis. The sections were immunostained according to standard protocols. Free-floating sections were incubated for 1–3 days at 4°C with primary antibody mixture diluted in TBS containing 0.1% Triton X-100 and 10% calf serum. The primary antibodies used are described in Table 1. Depending on the experiment, secondary antibodies included Cy3- or Cy2-conjugated anti-rabbit/mouse, Alexa488-conjugated anti-rabbit/mouse, Cy3- or Cy2-conjugated Streptavidin (Jackson Immunoresearch, Suffolk, UK), biotinylated anti-rabbit/mouse (Vector Laboratories, Servion, Switzerland), all used at the dilution recommended by the suppliers.

Stereotactic injections in mouse brains

The experiment was conducted essentially as already described [9, 13]. Briefly, AAV2/1.CAG.Flex.Tomato.WPRE.bGH viral construct (Vector Core, University of Pennsylvania, USA) was stereotactically injected in the brain of either *Slc17a6*::Cre or *Slc32a1*::Cre mice. Injections were performed in the NP^{Calb}, at the following Bregma coordinates: rostro-caudal: –6.36 mm, mediolateral: –0.2 mm, and dorso-ventral: –4.35 mm. Two weeks after the stereotactic injections, the animals were anesthetized

Table 1. Description of Primary Antibodies Used for Immunohistochemistry

Antibody to	Host species	Antigen	Manufacturer	Catalog number	Dilution used
Calbindin D-28K	Mouse	Whole chicken protein from gut	Swant, Marly, Swizerland	CB300	1–2,000
Calbindin D-28K	Rabbit	Recombinant rat calbindin D-28K	Swant, Marly, Swizerland	CB38	1–2,000
Cart	Rabbit	Rat Cart aa 55–102	Phoenix Pharmaceuticals,Karlsruhe, Germany	H-003-62	1–2,000
Nesfatin	Rabbit	Rat Nesfatin aa 1–82	Phoenix Pharmaceuticals, Karlsruhe, Germany	H-003-22	1–1,000
c-fos	Mouse	Recombinant human c-fos aa 1–380	Abcam, Cambridge, UK	ab208942	1–2,000
ChAT	Rabbit	Pig ChAT aa 150–250	Abcam, Cambridge, UK	ab178850	1–1,000

The antigen, host species, manufacturer, catalog number, and working dilution are given for all primary antibodies used in this study.

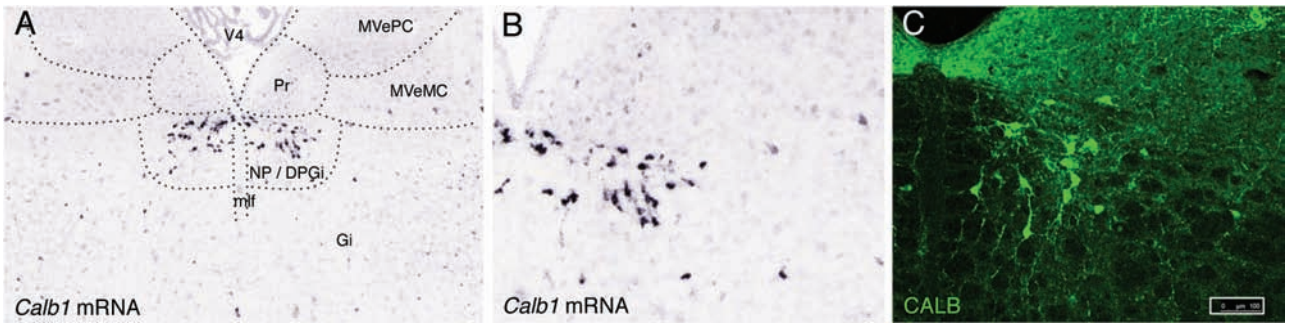

Figure 1. Expression of *Calb1* mRNA (A and B) and protein (C) in the NP^{Calb}. ISH images (A and B) were taken from the Allen Brain Atlas (Image credit: Allen Institute; http://mouse.brain-map.org/experiment/show/79556672). (B) It is a higher magnification of the image shown in (A), focusing only on one hemisphere. (C) It is a confocal image of a mouse brain coronal section immunostained for Calb protein, showing immunoreactivity in neuronal cell bodies within the DPGi and in neuritis in surrounding areas (Pr and Gi). DPGi, dorsal paragigantocellular nucleus; Gi, gigantocellular reticular nucleus; MVeMC, medial vestibular nucleus, magnocellular; MVePC, medial vestibular nucleus, parvicellular; NP, *Nucleus papilio*; Pr, *prepositus nucleus*; V4, fourth ventricle.

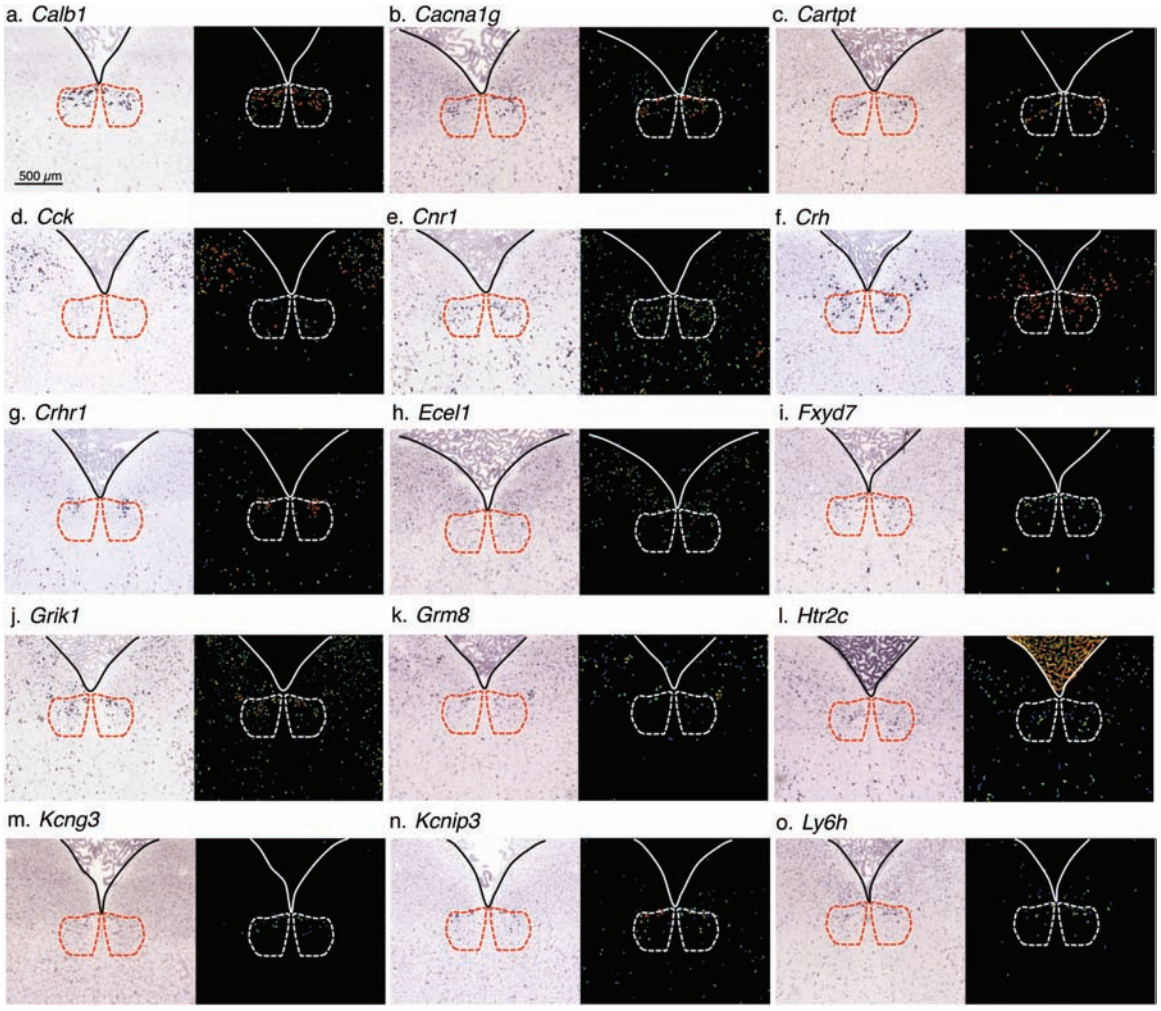

Figure 2. Genes showing expression in the area of the NP^{Calb}—Part 1. The expression profile of the following genes is shown: (A) *Calb1*, (B) *Cacna1g*, (C) *Cartpt*, (D) *Cck*, (E) *Cnr1*, (F) *Crh*, (G) *Crhr1*, (H) *Ecel1*, (I) *Fxyd7*, (J) *Grik1*, (K) *Grm8*, (L) *Htr2c*, (M) *Kcng3*, (N) *Kcnip3*, and (O) *Ly6h*. For the complete name of the genes shown, as well as the function of the encoded proteins, see Tables 1–3. Red, respectively white, dashed lines delimit the NP^{Calb} area. Black, respectively white, lines delimit the fourth ventricle. Data for the *Calb1* gene are given in panel (A) as reference. For each gene are shown both the ISH image (left; obtained with a digoxygenin-based method) and the corresponding colored image (right; ranging from blue to red, respectively from low to high expression) (Image credit: Allen Institute; *Calb1*: http://mouse.brain-map.org/experiment/show/79556672; *Cacna1g*: http://mouse.brain-map.org/experiment/show/71587822; *Cartpt*: http://mouse.brain-map.org/experiment/show/72077479; *Cck*: http://mouse.brain-map.org/experiment/show/200; *Cnr1*: http://mouse.brain-map.org/experiment/show/79591675; *Crh*: http://mouse.brain-map.org/experiment/show/292; *Crhr1*: http://mouse.brain-map.org/experiment/show/297; *Ecel1*: http://mouse.brain-map.org/experiment/show/70231305; *Fxyd7*: http://mouse.brain-map.org/experiment/show/73592536; *Grik1*: http://mouse.brain-map.org/experiment/show/75749751; *Grm8*: http://mouse.brain-map.org/experiment/show/73771227; *Htr2c*: http://mouse.brain-map.org/experiment/show/73636098; *Kcng3*: http://mouse.brain-map.org/experiment/show/71717451; *Kcnip3*: http://mouse.brain-map.org/experiment/show/71587887; *Ly6h*: http://mouse.brain-map.org/experiment/show/71924388).

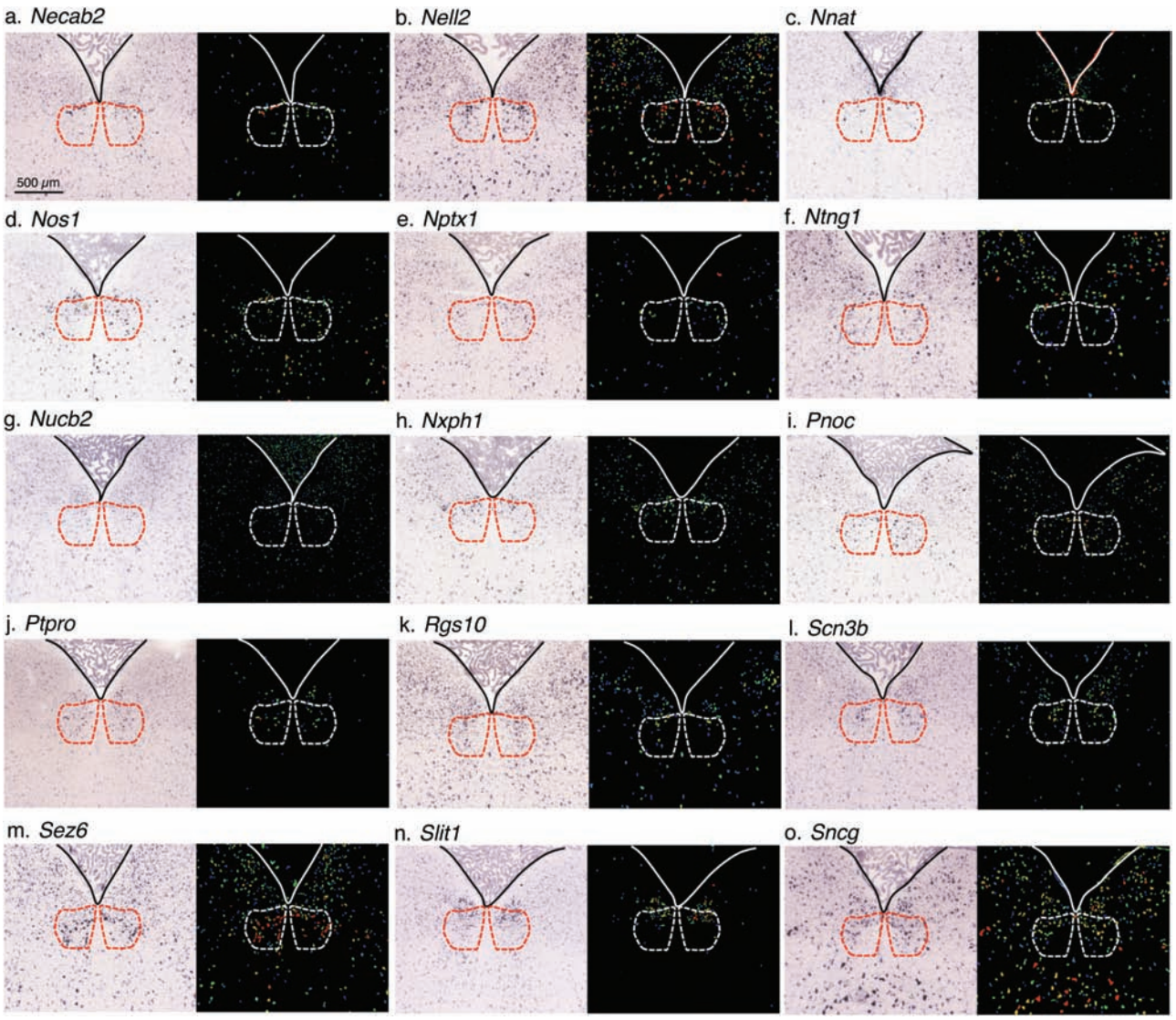

Figure 3. Genes showing expression in the area of the NP^{Calb}—Part 2. The expression profile of the following genes is shown: (A) *Necab2*, (B) *Nell2*, (C) *Nnat*, (D) *Nos1*, (E) *Nptx1*, (F) *Ntng1*, (G) *Nucb2*, (H) *Nxph1*, (I) *Pnoc*, (J) *Ptpro*, (K) *Rgs10*, (L) *Scn3b*, (M) *Sez6*, (N) *Slit1*, and (O) *Sncg*. See the legend of Figure 2 for details (Image credit: Allen Institute; *Necab2*: http://mouse.brain-map.org/experiment/show/73788010; *Nell2*: http://mouse.brain-map.org/experiment/show/72103854; *Nnat*: http://mouse.brain-map.org/experiment/show/77887874; *Nos1*: http://mouse.brain-map.org/experiment/show/75147762; *Nptx1*: http://mouse.brain-map.org/experiment/show/73520998; *Ntng1*: http://mouse.brain-map.org/experiment/show/71924185; *Nucb2*: http://mouse.brain-map.org/experiment/show/75774683; *Nxph1*: http://mouse.brain-map.org/experiment/show/75084479; *Pnoc*: http://mouse.brain-map.org/experiment/show/75038402; *Ptpro*: http://mouse.brain-map.org/experiment/show/72340109; *Rgs10*: http://mouse.brain-map.org/experiment/show/74511849; *Scn3b*: http://mouse.brain-map.org/experiment/show/71064082; *Sez6*: http://mouse.brain-map.org/experiment/show/71063725; *Slit1*: http://mouse.brain-map.org/experiment/show/73788105; *Sncg*: http://mouse.brain-map.org/experiment/show/72081426).

and perfused with 4% paraformaldehyde. The brains were excised and cryo-sectioned, and the specimens were analyzed immunohistochemically for Cart and Tomato expression. In these conditions, a specific and accurate Tomato expression is obtained in Cre-expressing neurons, as previously shown in *Calb1*::Cre mice [9].

REM sleep deprivation and rebound assay

Mice were deprived of REM sleep by implementing a modified version of the flower-pot technique, which spared the animals of major stress [14, 15]. Three groups were established: in the first group ("REM sleep deprivation and rebound" = *REMS-D + R*), the animals (n = 5) were maintained together for 72 h on six small stone platforms (7 × 4 cm for rats, 3 × 3 for mice), placed in a water tank. The surface of the platform was 1 cm above the water level. During this 72 h period, the animals had free access to food and water. Owing to the loss of the muscular tone that characterizes the onset of REM sleep, the animals fell into the water and were thereby deprived of REM sleep. After 72 h, the animals were transferred to a conventional cage in a quiet room and were permitted for 3 h to undergo REM sleep (=rebound). In the second group ("REM sleep deprivation" = *REMS-D*), the animals (n = 5) were sacrificed immediately after the termination of the 72 h REM sleep deprivation period, without recovery. In the third group ("control" = *C*), the animals (n = 5) were maintained in their cages under standard conditions for 72 h prior to sacrifice. The animals were anesthetized and perfused with

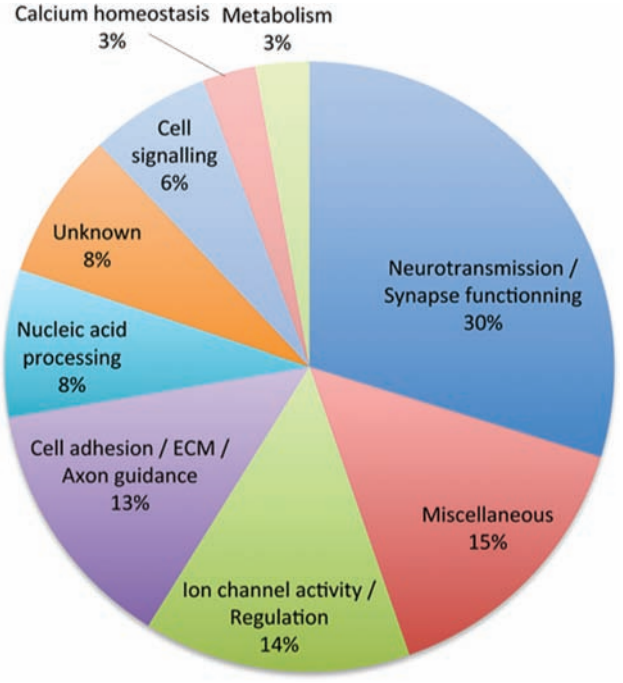

Figure 4. Proportions of the several categories of genes expressed in the NP^{Calb} area. See also Tables 1–3 for details on gene name and function.

fixative as described above under the "Animals" section. The brains were then excised and cryo-sectioned. The sections were immunostained for Cart as well as for c-fos, a surrogate marker of neuronal activity [16] The number of double-stained c-fos/Cart was determined on alternating 30 µm coronal sections, on the following brain areas: dorsal motor nucleus of vagus (10N)/nucleus of the solitary tract (Sol), *Nucleus prepositus* (Pr), DPGi, gigantocellular reticular nucleus (Gi), medial longitudinal fasciculus (mlf), and lateral paragigantocellular nucleus (LPGi). Only cells with strong Cart immunoreactivity were taken into account. The percentage of Cart+Fos+ relative to the total Cart+ cells was statistically compared between the three different conditions using a one-tailed Student's *t*-test, for each of the anatomical areas investigated. Data from $n = 4$ animals in each of the conditions were used.

Image analysis

The specimens were evaluated either in a Leica epifluorescence microscope, a Nikon Eclipse Ni fluorescence microscope, a Leica TCS SP5 confocal laser microscope, or a Hamamatsu Nanozoomer scanner. Postprocessing of the images and contrast adjustments therein were performed using the Adobe Photoshop and Nanozoomer slide-processing software.

Informatics

A search of the adult mouse ABA (https://portal.brain-map.org/) was undertaken to identify genes that might be coexpressed with *Calb1* in the targeted NP^{Calb}. First, we downloaded three-dimensional expression data measured by ISH from coronal sections of the adult mouse brain using ALLENMINER (v2.0) [10]. Since the *Calb1* gene expression in the target nucleus was restricted to a small region, we only used data from the coronal ISH series (4,216 datasets available for 3,968 genes), which are more densely sampled than the sagittal ones. Next, we defined a region of interest (ROI), which bilaterally encompassed the *Calb1*-expressing cells and the local neighborhood as a cube with boundaries in ABA coordinate space of 11–12 mm rostro-caudal, 5.4–6.4 mm dorso-ventral, and 5–6.4 mm medio-lateral. Within this ROI, the patterns of gene expression were then ranked relative to that for *Calb1* (ABA image series 71717640, https://mouse.brain-map.org/experiment/show/71717640 and 79556672, https://mouse.brain-map.org/experiment/show/79556672), as measured by the Pearson's correlation of the expression energy reported in corresponding voxels in the region (ALLENMINER run mode—sim search). An additional search was performed using the AGEA facility available at the ABA, allowing users to screen for genes expressed in a selected ROI [12]. The area investigated, focused on the DPGi, corresponded to AGEA coordinates: 11.154/5.422/5.887.

Results

Data mining for genes expressed in the Nucleus papilio in the mouse brain

The NP^{Calb} was previously defined as a symmetric cluster of Calb-expressing neurons, lodged in the DPGi, which in the mouse brain spans a distance of ~0.6 mm, from Bregma levels –5.8 to –6.4 mm [9]. The ABA ISH data available for the *Calb1* gene show that *Calb1* mRNA expression fully recapitulates the protein expression (Figure 1) [9, 17].

For the ALLENMINER search, we drew only on data that were derived from coronally sectioned ISH series (4,216 datasets available for 3,968 genes—see the "Methods" section). Consequently, they relate to only a fraction of the murine genome. Additional data mining using AGEA yielded 107 pages each comprising 20 genes, with ISH data also corresponding to coronal sections. The genes that were selected by both automated searches were further screened by visual inspection of the imaged ISH sections that traversed the NP^{Calb} area. After this second round of screening, we eliminated genes for which the signals were so low as to raise doubts respecting their specificity and those with ubiquitous expression in the *medulla oblongata*.

The screens identified 141 genes, which are restrictedly expressed in discrete regions of the *medulla oblongata*, including the area comprising the NP^{Calb}. Figures 2 and 3 illustrate examples of genes that manifest such restricted expression patterns, with a focus on the area corresponding to the NP^{Calb}. The genes fall into several main categories (Figure 4; Tables 2–4):

- "Neurotransmission": Neuropeptides: *Adcyap1*; *Cartpt*, *Cck*, *Crh*, *Nucb2*, *Nxph1*, *Nxph4*, *Penk*, *Pnoc*. Neurotransmitter/neuropeptide receptor: *Chrm2*, *Chrm3*, *Cnr1*, *Crhr1*, *Gabra1*, *Glra1*, *Glra4*, *Grid1*, *Grik1*, *Grin3a*, *Grm8*, *Htr2c*. Neurotransmitter synthesis/transport/release/exocytosis: *Apba1*, *Baiap3*, *Gad1*, *Gad2*, *Nos1*, *Nos1ap*; *Slc17a6*, *Slc17a7*, *Slc32a1*, *Sv2b*, *Sv2c*, *Syt4*.
- "Synapse functioning": *Cadps2*, *Nrn1*, *Ptpro*, *Sez6*, *Sez6l*, *Sv2b*, *Sv2c*.
- "Ion channel": For calcium: *Cacna1g*, *Cacna1h*, *Cacna2d1*, *Cacna2d3*, *Cacng5*. For potassium: *Hcn1*, *Kcna1*, *Kcnb1*, *Kcnc2*, *Kcnc3*, *Kcng3*, *Kcng4*, *Kcnj3*. For sodium: *Asic2*, *Scn3b*, *Scn4b*. Ion channel regulation: *Fxyd6*, *Fxyd7*, *Kcnip1*, *Kcnip4*.
- "Cell adhesion/Extracellular matrix/Axon guidance": *Ajap*, *Cdh8*, *Cdh13*, *Cd24a*, *Cntnap2*, *Col6a1*, *Col27a1*, *Crta1*, *Igsf21*, *Megf11*, *Nell2*, *Npnt*, *Ntng1*, *Sdk2*, *Sema3a*, *Sema6a*, *Slit1*, *Slit2*, *Spp1*.

Table 2. Genes Expressed in the DPGi/NP^{Calb} Region—Part 1

Gene	Complete name	Molecular activity	Biological process
Adarb1	Adenosine deaminase, RNA-specific, B1	Enzyme	Nucleic acid processing
Adcyap1	Adenylate cyclase activating polypeptide 1 (=PACAP)	Neuropeptide	Neurotransmission/synapse functioning (neuropeptide) [18, 19]
Adk	Adenosine kinase	Enzyme	Metabolism (adenine) [20]
Ajap1	Adherens junction associated protein 1 (=Shrew1)		Cell adhesion/ECM/axon guidance
Apba1	Amyloid beta (A4) precursor protein binding, family A, member 1 (=X11/Mint1)	Adaptator protein	Neurotransmission/synapse functioning (neurotransmitter release)
Arl10	ADP-ribosylation factor-like 10	GTPase activity	Multiple
Asic2	Acid-sensing (proton-gated) ion channel 2	Sodium channel	Ion channel
Baiap3	BAI1-associated protein 3		Neurotransmission/synapse functioning (SNARE-dependent exocytosis)
Btbd11	BTB (POZ) domain containing 11		
Cacna1g	Calcium channel, voltage-dependent, T type, alpha 1G subunit (=Cav3.1)	Calcium channel	Ion channel [21–23]
Cacna1h	Calcium channel, voltage-dependent, T type, alpha 1H subunit (=Cav3.2)	Calcium channel	Ion channel [21–23]
Cacna2d1	Calcium channel, voltage-dependent, alpha2/delta subunit 1 (=a2d1)	Calcium channel	Ion channel
Cacna2d3	Calcium channel, voltage-dependent, alpha2/delta subunit 3 (=a2d3)	Calcium channel	Ion channel
Cacng5	Calcium channel, voltage-dependent, gamma subunit 5	Calcium channel	Ion channel
Cadps2	Ca2+-dependent activator protein for secretion 2		Neurotransmission/synapse functioning (dendritic spine maintenance)
Calb1	Calbindin 1 (=Calbindin D28k)	EF-hand Ca binding; calcium sensor/buffer	Calcium homeostasis [9]
Calb2	Calbindin 2 (=Calretinin)	EF-hand Ca binding; calcium sensor/buffer	Calcium homeostasis
CamkV	CaM kinase-like vesicle-associated	Enzyme	Neurotransmission/synapse functioning
Cartpt	CART prepropeptide	Neuropeptide	Neurotransmission/synapse functioning (neuropeptide) [24–26]
Cck	Cholecystokinin	Neuropeptide	Neurotransmission/synapse functioning (neuropeptide) [27, 28]
Cdh8	Cadherin 8	Protein binding	Cell adhesion/ECM/axon guidance
Cdh13	Cadherin 13 (=Tcad)	Protein binding	Cell adhesion/ECM/axon guidance
Cd24a	CD24a antigen	Protein binding	Cell adhesion/ECM/axon guidance
Chrm2	Cholinergic receptor, muscarinic 2, cardiac (=AChR-M2)	GPCR	Neurotransmission/synapse functioning (cholinergic receptor) [29–31]
Chrm3	Cholinergic receptor, muscarinic 3, cardiac (=AChR-M3)	GPCR	Neurotransmission/synapse functioning (cholinergic receptor) [29–31]
Cnr1	Cannabinoid receptor 1 (brain) (=CB1)	GPCR	Neurotransmission/synapse functioning (cannabinoid receptor) [32, 33]
Cntnap2	Contactin associated protein-like 2 (=Caspr2)	Protein binding	Cell adhesion/ECM/axon guidance [34]
Coch	Cochlin	Protein binding	Immunity
Col6a1	Collagen, type VI, alpha 1	ECM structural component	Cell adhesion/ECM/axon guidance
Col27a1	Procollagen, type XXVII, alpha 1	ECM structural component	Cell adhesion/ECM/axon guidance
Cpne6	Copine VI	Ca binding; Ca sensor	Neurotransmission/synapse functioning
Crh	Corticotropin releasing hormone	Neuropeptide	Neurotransmission/synapse functioning (neuropeptide) [35]
Crhr1	Corticotropin releasing hormone receptor 1	GPCR	Neurotransmission/synapse functioning (neuropeptide receptor)
Crtac1	Cartilage acidic protein 1 (=Lotus)	Ca binding; protein binding	Cell adhesion/ECM/axon guidance
Ctxn1	Cortexin 1		
Cux2	Cut-like homeobox 2	Transcription factor	Nucleic acid processing
Cyp26b1	Cytochrome P450, family 26, subfamily b, polypeptide 1	Enzyme	Metabolism
Deptor	DEP domain containing MTOR-interacting protein (=Depdc6)		Cell signaling
Dkk3	Dickkopf WNT signaling pathway inhibitor 3	Secreted ligand	Cell signaling
Dpp10	Dipeptidylpeptidase 10	Enzyme	Proteolysis
Ecel1	Endothelin converting enzyme-like 1	Enzyme	Multiple
Esyt1	Extended synaptotagmin-like protein 1	Ca/lipid/protein binding	Intracellular lipid dynamics
Fbxw7	F-box and WD-40 domain protein 7	Protein binding	Cell signaling
Foxa1	Forkhead box A1	Transcription factor	Nucleic acid processing
Foxp1	Forkhead box P1	Transcription factor	Nucleic acid processing
Fxyd6	FXYD domain-containing ion transport regulator 6	Na-K ATPase regulator	Ion channel regulation
Fxyd7	FXYD domain-containing ion transport regulator 7	Na-K ATPase regulator	Ion channel regulation

A list of the genes that are restrictedly expressed in discrete regions of the murine *medulla oblongata*, including the region embracing the *Nucleus papilio*, as revealed by ALLENMINER and AGEA searches of the ISH images in the ABA. The abbreviated as well as the full name of each gene are given, together with their known or putative molecular activity and functions (in ontologic terms). In gray: genes that have been experimentally implicated in the regulation of the sleep/wake cycle, with references indicated.

Table 3. Genes Expressed in the DPGi/NP^{Calb} Region—Part 2 (see the footnote of Table 2)

Gene	Complete name	Molecular activity	Biological process
Gabra1	Gamma-aminobutyric acid (GABA) A receptor, subunit alpha 1	Transmitter gated ion channel activity	Neurotransmission/synapse functioning (GABA receptor)
Gad1	Glutamic acid decarboxylase 1	Enzyme	Neurotransmission/synapse functioning (GABA synthesis)
Gad2	Glutamic acid decarboxylase 2	Enzyme	Neurotransmission/synapse functioning (GABA synthesis)
Glra1	Glycine receptor, alpha 1 subunit	Transmitter gated ion channel activity	Neurotransmission/synapse functioning (glycine receptor)
Glra4	Glycine receptor, alpha 4 subunit	Transmitter gated ion channel activity	Neurotransmission/synapse functioning (glycine receptor)
Gpr125	G protein-coupled receptor 125 (=Adgra3)	GPCR	Cell signaling
Gpr137	G protein-coupled receptor 137	GPCR	Cell signaling
Grid1	Glutamate receptor, ionotropic, delta 1	Transmitter gated ion channel activity	Neurotransmission/synapse functioning (glutamate receptor)
Grik1	Glutamate receptor, ionotropic, kainate 1	Transmitter gated ion channel activity	Neurotransmission/synapse functioning (kainate/glutamate receptor)
Grin3a	Glutamate receptor ionotropic, NMDA3A	Transmitter gated ion channel activity	Neurotransmission/synapse functioning (NMDA/glutamate receptor)
Grm8	Glutamate receptor, metabotropic 8	GPCR	Neurotransmission/synapse functioning (glutamate receptor)
Grsf1	G-rich RNA sequence binding factor 1	RNA binding	Nucleic acid processing
Gsta4	Glutathione S-transferase, alpha 4	Enzyme	Metabolism (glutathione metabolism)
Hap1	Huntingtin-associated protein 1	Protein binding	Axonal transport
Hcn1	Hyperpolarization-activated, cyclic nucleotide-gated K^+ 1	Potassium channel	Ion channel
Htr2c	5-Hydroxytryptamine (serotonin) receptor 2C	GPCR	Neurotransmission/synapse functioning (serotonin receptor) [36]
Igsf21	Immunoglobulin superfamily, member 21	Protein binding	Cell adhesion/ECM/axon guidance
Itm2c	Integral membrane protein 2C		
Kcna1	Potassium voltage-gated channel, shaker-related subfamily, member 1 (=Kv1.1)	Potassium channel	Ion channel
Kcnab1	Potassium voltage-gated channel, shaker-related subfamily, beta member 1 (=Kv1.3)	Potassium channel	Ion channel
Kcnc2	Potassium voltage gated channel, Shaw-related subfamily, member 2 (=Kv3.2)	Potassium channel	Ion channel [37]
Kcnc3	Potassium voltage gated channel, Shaw-related subfamily, member 3 (=Kv3.3)	Potassium channel	Ion channel [38]
Kcng3	Potassium voltage-gated channel, subfamily G, member 3 (=Kv6.3)	Potassium channel	Ion channel
Kcng4	Potassium voltage-gated channel, subfamily G, member 4 (=Kv6.4)	Potassium channel	Ion channel
Kcnj3	Potassium inwardly rectifying channel, subfamily J, member 3	Potassium channel	Ion channel
Kcnip1	Kv channel-interacting protein 1 (=KCHIP1)	K channel regulator (Ca binding)	Ion channel regulation
Kcnip4	Kv channel interacting protein 4 (=KCHIP4)	K channel regulator (Ca binding)	Ion channel regulation
Lrrn1	Leucine rich repeat protein 1, neuronal		
Ly6h	Lymphocyte antigen 6 complex, locus H	Prototoxin	Neurotransmission/synapse functioning (modulation of AchR activity)
Megf11	Multiple EGF-like-domains 11		Cell adhesion/ECM/axon guidance
Mesdc2	Mesoderm development candidate 2	Chaperone LDL	Cell signaling
Myo5b	Myosin VB	Multiple	Cytoskeleton dynamics
Ndst4	N-deacetylase/N-sulfotransferase (heparin glucosaminyl) 4	Enzyme	Metabolism (glycosaminoglycan)
Necab2	N-terminal EF-hand calcium binding protein 2	EF-hand Ca binding	
Necab3	N-terminal EF-hand calcium binding protein 3	EF-hand Ca binding	
Nell2	NEL-like 2 (neural EGF like 2)	Ca/protein/ECM binding	Cell adhesion/ECM/axon guidance
Nnat	Neuronatin		Multiple
Nos1	Nitric oxide synthase 1, neuronal	Enzyme	Neurotransmission/synapse functioning (NO synthesis) [39–41]
Nos1ap	Nitric oxide synthase 1 (neuronal) adaptor protein (=Capon)	Protein binding	Neurotransmission/synapse functioning (NO synthesis)
Npnt	Nephronectin	Ca/protein/ECM binding	Cell adhesion/ECM/axon guidance
Nptx1	Neuronal pentraxin 1 (=NP1)		Neurotransmission/synapse functioning
Nrg1	Neuregulin 1	Protein binding	Cell signaling
Nrn1	Neuritin 1		Neurotransmission/synapse functioning
Ntng1	Netrin G1	Protein binding	Cell adhesion/ECM/axon guidance
Nucb2	Nucleobindin 2	Ca2+/DNA binding/neuropeptide	Neurotransmission/synapse functioning (neuropeptide) [42, 43]
Nxph1	Neurexophilin 1	Neurexin ligand	Neurotransmission/synapse functioning (neuropeptide-like)
Nxph4	Neurexophilin 4	Neurexin ligand	Neurotransmission/synapse functioning (neuropeptide-like)

Table 4. Genes Expressed in the DPGi/NP^{Calb} Region—Part 3 (see the footnote of Table 2)

Gene	Complete name	Molecular activity	Biological process
Pcp4	Purkinje cell protein 4	Ca/protein binding	Multiple
Pcp4l1	Purkinje cell protein 4-like 1	Ca/protein binding	Multiple
Penk	Preproenkephalin	Neuropeptide	Neurotransmission/synapse functioning (neuropeptide)
Pnoc	Prepronociceptin	Neuropeptide	Neurotransmission/synapse functioning (neuropeptide)
Psd	Pleckstrin and Sec7 domain containing (=EFA6)	GEF activity	Axonal transport
Ptpro	Protein tyrosine phosphatase, receptor type, O	Receptor/enzyme	Neurotransmission/synapse functioning (promotes synapse formation)
Pvalb	Parvalbumin	EF-hand Ca binding; calcium sensor/buffer	Calcium homeostasis [44]
Rec8	REC8 meiotic recombination protein	Chromatin binding	Nucleic acid processing
Rgs4	Regulator of G-protein signaling 4	GTPase activator	Cell signaling
Rgs10	Regulator of G-protein signaling 10	GTPase activator	Cell signaling
Scn3b	Sodium channel, voltage-gated, type III, beta	Sodium channel	Ion channel
Scn4b	Sodium channel, type IV, beta	Sodium channel	Ion channel
Scrt1	Scratch family zinc finger 1	Transcription repressor	Nucleic acid processing
Sdk2	Sidekick homolog 2 (chicken)		Cell adhesion/ECM/axon guidance
Slc6a7	Solute carrier family 6 (neurotransmitter transporter, L-proline), member 7	Proline transporter	Multiple
Slc8a1	Solute carrier family 8 (sodium/calcium exchanger), member 1 (=Ncx1)	Ca/Na antiporter	Calcium homeostasis
Slc17a6	Solute carrier family 6 (sodium-dependent inorganic phosphate cotransporter), member 6	Vesicular neurotransmitter transporter	Neurotransmission/synapse functioning (=VGlut2, glutamate transporter)
Slc17a7	Solute carrier family 6 (sodium-dependent inorganic phosphate cotransporter), member 7	Vesicular neurotransmitter transporter	Neurotransmission/synapse functioning (=VGlut1, glutamate transporter)
Slc32a1	Solute carrier family 32 (GABA vesicular transporter), member 1	Vesicular neurotransmitter transporter	Neurotransmission/synapse functioning (=VGAT, GABA transporter)
Slc36a1	Solute carrier family 36 (proton/amino acid symporter), member 1	Transmembrane transporter	Multiple
Sema3a	Semaphorin 3A	Protein/ECM binding	Cell adhesion/ECM/axon guidance
Sema6a	Semaphorin 6a	Protein/ECM binding	Cell adhesion/ECM/axon guidance
Sez6	Seizure related gene 6 (=BSRP-C)		Neurotransmission/synapse functioning (shaping dendritic arborization)
Sez6l	Seizure related 6 homolog like		Neurotransmission/synapse functioning (shaping dendritic arborization)
Sh3bgrl2	SH3 domain binding glutamic acid-rich protein like 2		
Slit1	Slit guidance ligand 1	Ca/protein/ECM binding	Cell adhesion/ECM/axon guidance
Slit2	Slit guidance ligand 2	Ca/protein/ECM binding	Cell adhesion/ECM/axon guidance
Snca	Synuclein, alpha	Protein binding	Multiple (involved in synucleinopathies including PD; RBD) [45, 46]
Sncg	Synuclein, gamma	Protein binding	Multiple
Sphkap	SPHK1 interactor, AKAP domain containing (=SKIP)	A kinase anchoring protein	
Spp1	Secreted phosphoprotein 1 (=OPN)	Cytokine/ECM binding	Cell adhesion/ECM/axon guidance
Steap2	Six transmembrane epithelial antigen of prostate 2	Enzyme	Multiple
Sv2b	Synaptic vesicle glycoprotein 2 b	Transmembrane transporter	Neurotransmission/synapse functioning (vesicular transport/exocytosis)
Sv2c	Synaptic vesicle glycoprotein 2c	Transmembrane transporter	Neurotransmission/synapse functioning (vesicular transport/exocytosis)
Syt4	Synaptotagmin IV	Ca/protein/lipid binding	Neurotransmission/synapse functioning (vesicular transport/exocytosis)
S100a10	S100 calcium-binding protein A10 (=calgizzarin)	EF-hand Ca binding/protein binding	Multiple
S100b	S100 protein, beta polypeptide, neural	EF-hand Ca binding/protein binding	Multiple (marker in sleep disturbance syndromes and PD)
Tesc	Tescalcin	EF-hand Ca binding/protein binding	Multiple
Tmem65	Transmembrane protein 65		
Tpbg	Trophoblast glycoprotein		
Usp11	Ubiquitin-specific peptidase 11	Enzyme	Proteolysis
Vat1l	Vesicle amine transport protein 1 homolog-like		
Whrn	Whirlin		Cytoskeleton dynamics
Zfp385b	Zinc finger protein 385B	Transcription factor	Nucleic acid processing
Zfhx4	Zinc finger homeodomain 4	Transcription factor	Nucleic acid processing
Zfp365	Zinc finger protein 365	Transcription factor	Nucleic acid processing
Zkscan16	Zinc finger with KRAB and SCAN domains 16	Transcription factor	Nucleic acid processing

- "Nucleic acid processing": *Adarb1*, *Cux2*, *Foxa1*, *Foxp1*, *Grsf1*, *Rec8*, *Scrt1*, *Zfp365*, *Zfp385b*, *Zfhx4*, *Zkscan16*.

Some other less represented categories included metabolism, cell signaling, and calcium homeostasis.

Identifying neurotransmitters and neuropeptides expressed in the Nucleus papilio

We have started previously to investigate the neurotransmitter status of NP^{Calb} neurons, by showing that a significant proportion (33.8%) of Calb-positive neurons were glutamatergic and that none were GABAergic [9]. Analyzing the ABA ISH data on sagittal sections revealed that the *Slc6a5* gene, encoding the Glyt2 glycine vesicular transporter, and the *Chat* gene, encoding choline acetyltransferase, were also expressed in the region of the *medulla oblongata*. Immunostaining for Calb on coronal sections from GlyT2-GFP mouse brain revealed that NP^{Calb} neurons were not glycinergic (Figure 5A–C′). Similarly, double immunostaining for Calb and Chat revealed the absence of Chat expression in NP^{Calb} neurons (Figure 5D–F′).

Our search identified several genes encoding neuropeptides that are likely to be coexpressed with *Calb1*, namely, *Cartpt* (encoding Cart, cocaine-and-amphetamine-regulated transcript), *Cck* (encoding cholecystokinin), *Crh* (encoding corticotrophin-releasing hormone), *Nucb2* (encoding nesfatin 1), *Penk* (encoding preproenkephalin), and *Pnoc* (encoding prepronociceptin) (see Figures 2 and 3 for the ABA ISH data). For the immunohistochemical revelation of coexpression, coronal sections through murine brains were double-stained for Calb and two of these neuropeptides. Nesfatin immunoreactivity was present in all Calb-immunoreactive neurons of the NP^{Calb} (Figure 6A–C and A′–C′), whereas that for Cart (Figure 6D–F and D′–F′) was apparent in some, but not all. In addition, some cells lying close to the Calb-immunoreactive neurons were positive for each of the tested peptides, but not for Calb. Noteworthy, similar observations were made using sections from rat brains (not shown). We estimated that 27.2% ± 5.6% of the DPGi Calb+ cells were Cart+ (counting performed on each second sections in n = 8 mice) and that 65.9% ± 13.7% of the DPGi Cart+ cells were Calb+ (counting performed in n = 3 mice).

Cart-expressing neurons within the DPGi are glutamatergic

With the aim of analyzing the neurotransmitter status of the Cart-expressing neurons in the NP^{Calb}/DPGI area, glutamatergic, respectively GABAergic, neurons within the *medulla oblongata* were labeled by means of fluorescent adenovirus tracer injection in *Slc17a6*::Cre mouse brains (encoding the VGlut2 glutamate transporter) and *Slc32a1*::Cre (encoding the VGAT GABA transporter). In these conditions, glutamatergic, respectively GABAergic, cell bodies could be easily identified by their strong fluorescence. Co-staining with anti-Cart antibody revealed that *all* Cart-positive cells within the DPGi were VGlut2-positive and that *none* was VGat-positive, highlighting their glutamatergic nature (Figure 7). In addition, Cart-positive cells located in either the adjacent *Nucleus prepositus* or the gigantocellular reticular nucleus were also mostly glutamatergic, while only very few Cart-positive cells within the *Nucleus prepositus* appeared as GABAergic.

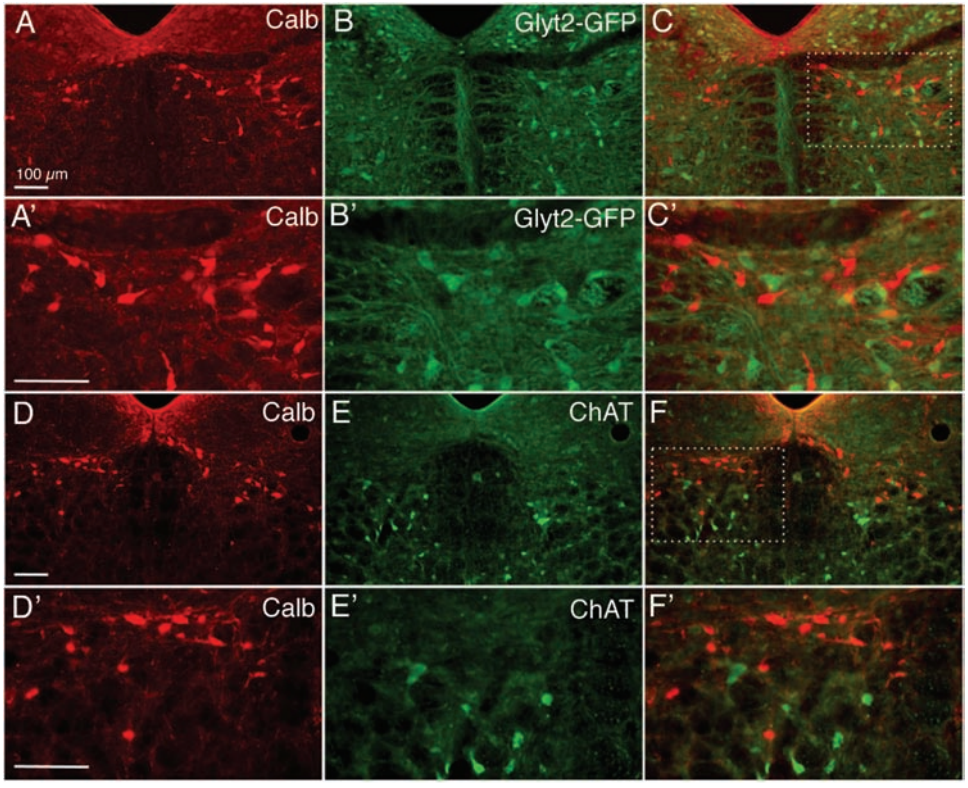

Figure 5. NP^{Calb} neurons are neither glycinergic nor cholinergic. (A–C′) Coronal sections from a GlyT2-GFP mouse brain, stained for Calb (red) and GFP (green). The dashed square in (C) marks the area shown at higher magnification in panels (A′–C′). (D–F′) Coronal sections from a C57Bl6 mouse brain, stained for Calb (red) and ChAT (green). The dashed square in (F) marks the area shown at higher magnification in panels (D′–F′). Bars represent 100 µm.

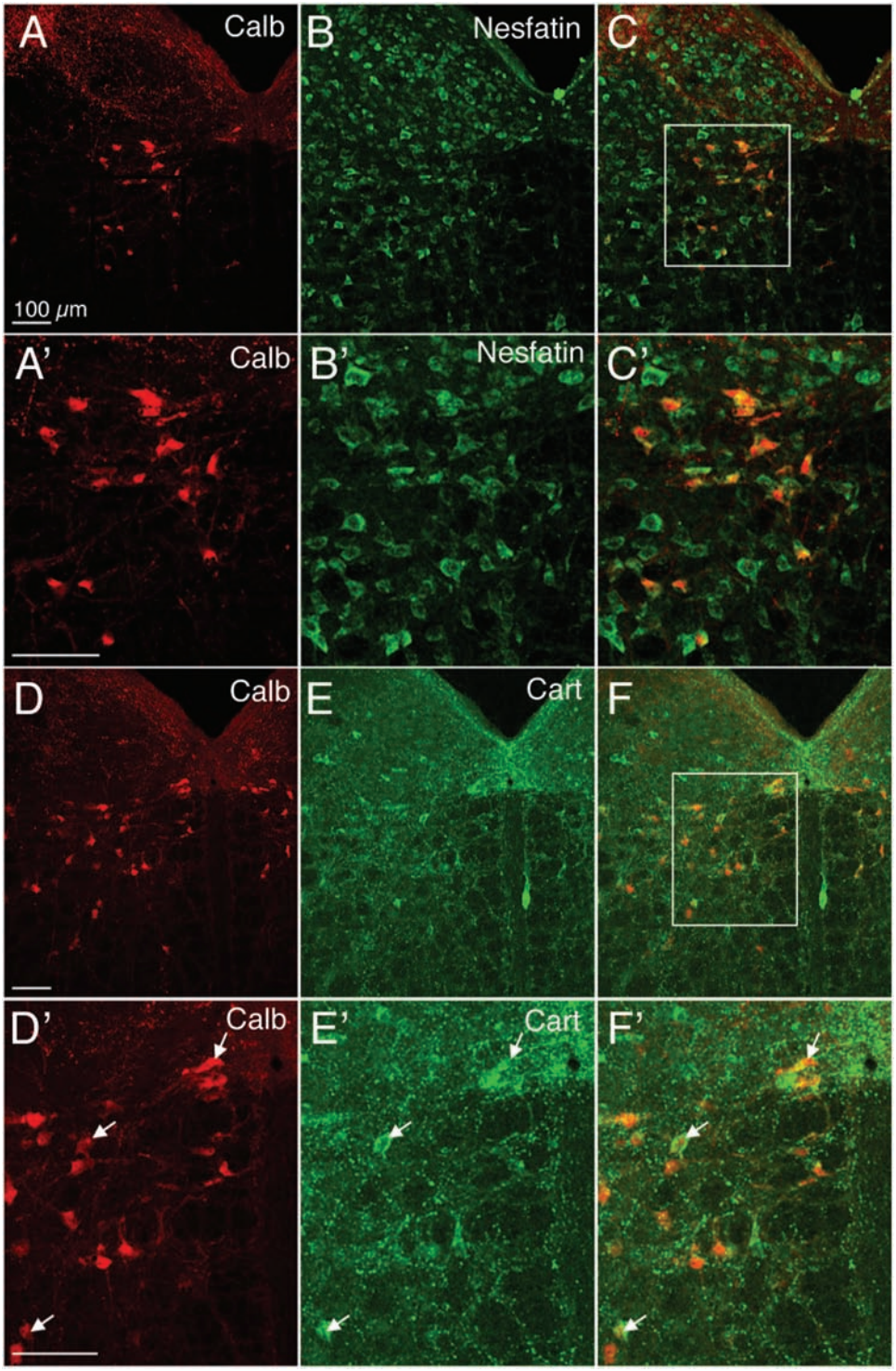

Figure 6. Cart and Nesfatin neuropeptide expression in NP^{Calb} neurons. Coronal sections from a C57Bl6 mouse brain, stained for Calb and either Nesfatin (A–C) or Cart (D–F) in the NP^{Calb}. All Calb-positive NP^{Calb}-neurons coexpress Nesfatin, while coexpression with Cart is limited to few neurons (marked by arrows in D′–F′). Panels (A′–C′) and (D′–F′) are higher magnifications. All images were obtained with confocal microscope. Bars represent 100 μm.

Cart-expressing neurons within the DPGi are activated during REM sleep

In an experimental paradigm consisting of REM sleep rebound following a 72 h REM sleep deprivation, we could demonstrate that neurons of the DPGi [47–49], and particularly the NP^{Calb} neurons [9], were activated during REM sleep, as demonstrated by neuronal c-fos immunoreactivity. A similar test performed on mice revealed that Cart-positive neurons localized within the DPGi of the *medulla oblongata* were activated during REM sleep too. Only in the DPGi significant differences between the three different groups analyzed could be observed (REM sleep deprivation group; REM sleep deprivation + rebound group; Control group) (Figure 8).

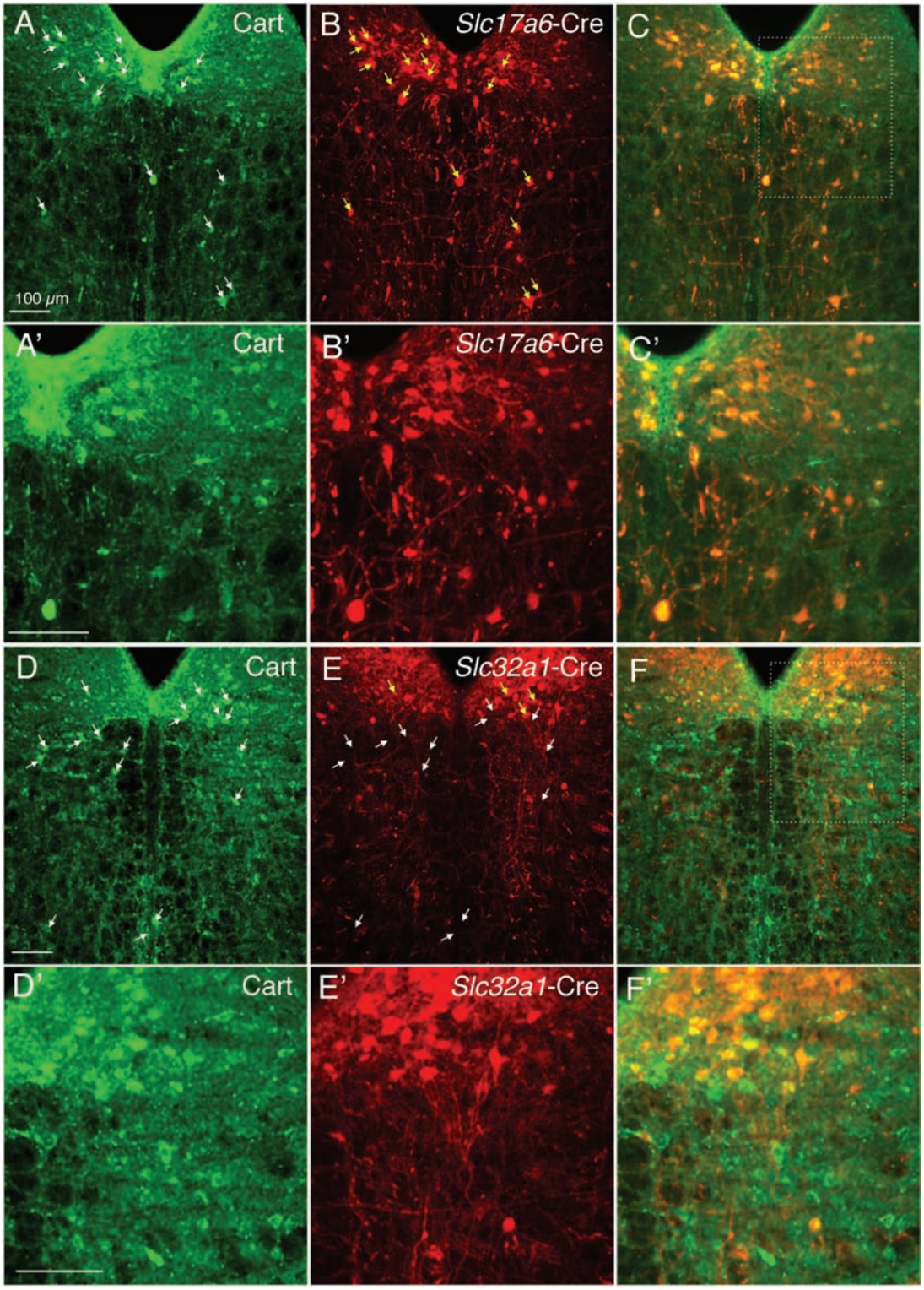

Figure 7. Cart-expressing neurons within the DPGi are glutamatergic. Immunostaining with Cart antibody reveals the glutamatergic nature of all Cart-expressing neurons in the DPGI. Shown are representative coronal sections through the *medulla oblongata* of a brain from (A–C′) *Slc7a6*::Cre (VGlut2-Cre) and (D–F′) *Slc32a1*::Cre (VGAT-Cre) mice, injected with Cre-dependent AAV-Tomato. In (C), respectively (F), a dashed square indicates the area presented at higher magnification in (A′–C′), respectively (D′–F′). White arrows in (A) and (D) point to Cart+ cells. Within the DPGi and the Gi, all Cart+ neurons are glutamatergic (yellow arrows in B), while none are GABAergic (white arrows in E). On the contrary, in the *prepositus nucleus* both glutamatergic and GABAergic Cart+ neurons are visible (yellow arrows pointing to Pr neurons in B and E). Bars represent 100 μm.

Indeed, in the REM sleep rebound group, we quantified 41.6% ± 6.9% of DPGi Cart-positive neurons displaying c-fos immunoreactivity and 31% ± 6.5% of DPGi c-fos+ cells being Cart+. Analyzing the other areas (including the Gi, the LPGi, the mlf, the 10N/Sol), no significant difference between the three groups was observed (Figure 8). This experiment suggests that Cart-expressing neurons in the DPGi are activated during the REM phase of sleep.

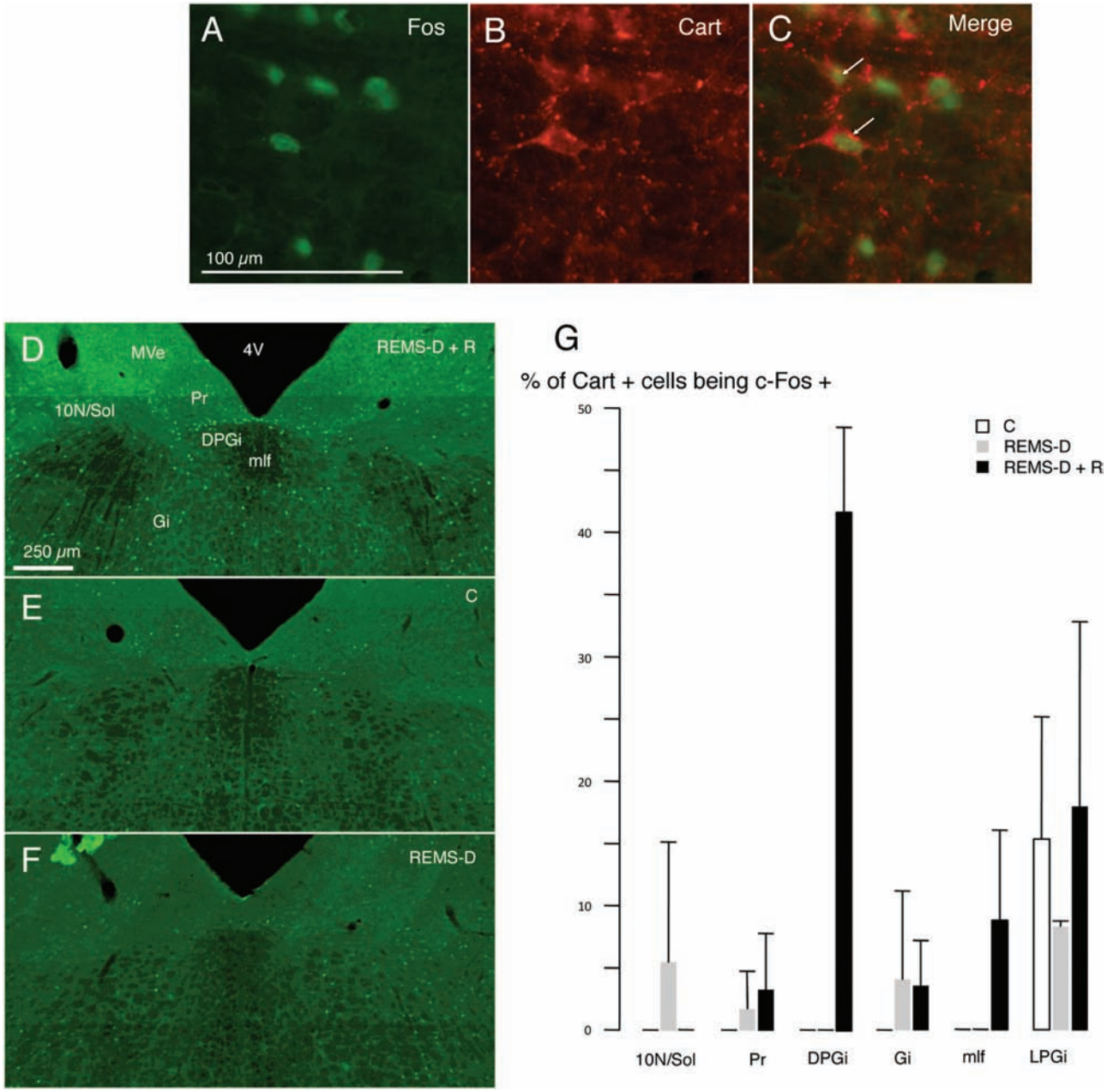

Figure 8. Analysis of c-fos immunoreactivity in Cart-expressing neurons in the *medulla oblongata* during REM sleep. (A–C) Representative coronal section from the brain of an animal of the group "REM sleep deprivation and rebound," stained for Cart (red) and c-fos (green). The two arrows in panel C point to Cart+c-fos+ neurons. (D–F) Representative brain coronal sections from animals of each three groups used for the REM sleep deprivation and rebound assay (REMSD + R, REM sleep deprivation and rebound; REMSD, REM sleep deprivation; C, Control), immunostained for c-fos. (G) Percentage of c-fos immunoreactive cells within the Cart+ population, in different brain areas. Counting was performed on alternating coronal sections from three animals of each three groups (REMSD + R; REMSD; C). Statistical significance at $p < 0.05$ between the different groups was achieved only in the DPGi; group REMS-D+R versus group C: $t = 10.78389$ and $p = 0.000019$; group REMS-D+R versus group REMS-D: $t = 10.78389$ and $p = 0.000019$. DPGi, dorsal paragigantocellular nucleus; Gi, gigantocellular reticular nucleus; LPGi, lateral paragigantocellular nucleus; mlf, medial longitudinal fasciculus; MVe, medial vestibular nucleus; Pr, *prepositus nucleus*; 4V, fourth ventricle; 10N, dorsal motor nucleus of vagus/Sol: nucleus of the solitary tract.

Discussion

The *Nucleus papilio* is a recently described brainstem structure, characterized by Calb immunoreactivity, and by its involvement in triggering eye movement during the REM sleep period [9]. Through an extensive data mining of the ABA, we propose here a list of genes that are likely to be expressed in the NP^{Calb}. Several of these genes encode proteins involved in the synthesis/transport of neurotransmitters, namely, *Slc17a7* and *Slc17a6* (encoding VGlut1- and VGlut2-glutamate transporter, respectively), *Gad1/2* (encoding glutamic acid decarboxylase, which is responsible for the production of GABA), and *Slc32a1* (encoding a GABA transporter). By injecting Cre-dependent AAV-Tomato virus in *Slc17a6*::Cre and *Slc17a7*::Cre (both specific for glutamatergic neurons) and *Slc32a1*::Cre mice (specific for GABAergic neurons), we were able to show the absence of Calb immunoreactivity in the GABAergic neurons of the DPGi, whereas a significant proportion of the Calb-positive neurons composing the NP^{Calb} were of glutamatergic nature [9]. Analyzing the list of potential genes expressed in the NP^{Calb}, several glutamate receptors and a single GABA receptor were found (Tables 2–4).

Of special interest for us were the genes encoding neuropeptides. Nesfatin 1 is derived from a precursor, nucleobindin 2, which via posttranslational cleavage, yields either the neuropeptide nesfatin 1 or the DNA/Ca^{2+}-binding proteins nesfatin 2 and 3. Nesfatin 1 has been identified as a satiety molecule in the hypothalamus [50]. Albeit so, its widespread extra-hypothalamic expression indicates that it might exert endocrine and autonomic effects on energy expenditure [51]. Cart peptides have been implicated in the regulation not only of food intake and body weight, but also of a variety of physiological processes, including drug reward/reinforcement and stress [52, 53], findings that are consistent with the complex pattern of Cart immunoreactivity in the rat brain [54]. Cart has been shown to coexist with Calb-D28k in granule cells of the dentate gyrus [55] and to be coexpressed with nesfatin in several hypothalamic and non-hypothalamic areas of the rat brain [51, 56, 57], including MCH-neurons. Data presented in the present study indicate that both peptides are coexpressed also in some Calb-immunoreactive neurons of the NP^{Calb}. Several studies that have been recently conducted afford evidence for a role of nesfatin 1 in the regulation of REM sleep. Disruption of nesfatin signaling in the tuberal hypothalamic neurons, by the intra-cerebroventricular administration of either an antiserum against the neuropeptide or *Nucb2* antisense, has been shown to suppress REM sleep [24]. Similarly, deprivation of REM sleep led to a downregulation of nesfatin 1 expression, which was reverted during REM rebound [25]. And finally, the activity of these hypothalamic nesfatin-positive neurons (which are also MCH positive), as monitored by c-fos immunostaining, was correlated with REM sleep [24, 25]. Clear evidence in favor of an involvement of Cart in the regulation of the sleep/wake regulation has not been forthcoming [26]. Indeed, although an intra-cerebroventricular injection of the Cart55-102-peptide promotes the wake phase in rats [18], both Cart-positive and Cart-negative MCH-immunoreactive neurons in the hypothalamus are activated during REM sleep [19, 20]. Our finding that a significant proportion of Cart-expressing neurons in the DPGi were c-fos-positive following REM sleep rebound is thus particularly interesting and suggests a possible involvement of Cart in regulating some aspects of REM sleep.

The Calb-expressing neurons forming the NP^{Calb} appear to form a heterogeneous population, involved partly in controlling eye movement during REM sleep [9], with a substantial number being excitatory glutamatergic neurons, and with the neuropeptides Cart and nociceptin being expressed only in a subset of these neurons while nesfatin being present in all of them (this study). In addition, the surrounding DPGi also contains another pool of inhibitory GABAergic neurons involved in the initiation of REM sleep, as well as glycinergic and cholinergic neurons [4, 7, 8]. Deciphering the specific neuronal connections made by these particular neuronal populations will be challenging toward a better understanding of the functions of this nucleus in regulating various aspects of REM sleep. Indeed, apart from their connections to the three eye motor nuclei, we observed strong efferent connections of the NP^{Calb} neurons to several of the brain areas involved in the initiation and the maintenance of REM sleep (including the subcoeruleus nucleus and the pontine reticular nuclei) [9], suggesting additional roles for the NP^{Calb} in regulating some aspects of REM sleep.

Acknowledgments

We thank Simone Eichenberger, Drs Viktoria Szabolcsi, and Diana Waldmeyer-Roccaro for their technical assistance. We thank Dr Zeilhofer for the kind gift of GlyT2-GFP mice.

Funding

This work was funded by the Canton of Fribourg (Switzerland) and the Swiss National Foundation (31003A-144036 and 320030-179565).

Disclosure Statement

Financial disclosure: none.
Nonfinancial disclosure: none.

References

1. Peever J, *et al*. The biology of REM sleep. *Curr Biol*. 2017;**27**(22):R1237–R1248.
2. Reinoso-Suárez F, *et al*. Brain structures and mechanisms involved in the generation of REM sleep. *Sleep Med Rev*. 2001;**5**(1):63–77.
3. Brown RE, *et al*. Control of sleep and wakefulness. *Physiol Rev*. 2012;**92**(3):1087–1187.
4. Luppi PH, *et al*. Paradoxical (REM) sleep genesis by the brainstem is under hypothalamic control. *Curr Opin Neurobiol*. 2013;**23**(5):786–792.
5. Weber F, *et al*. Circuit-based interrogation of sleep control. *Nature*. 2016;**538**(7623):51–59.
6. Scammell TE, *et al*. Neural circuitry of wakefulness and sleep. *Neuron*. 2017;**93**(4):747–765.
7. Goutagny R, *et al*. Role of the dorsal paragigantocellular reticular nucleus in paradoxical (rapid eye movement) sleep generation: a combined electrophysiological and anatomical study in the rat. *Neuroscience*. 2008;**152**(3):849–857.
8. Clément O, *et al*. The inhibition of the dorsal paragigantocellular reticular nucleus induces waking and the activation of all adrenergic and noradrenergic neurons: a combined pharmacological and functional neuroanatomical study. *PLoS One*. 2014;**9**(5):e96851.
9. Gutierrez Herrera C, *et al*. Neurons in the Nucleus papilio contribute to the control of eye movements during REM sleep. *Nat Commun*. 2019;**10**(1):5225.
10. Davis FP, *et al*. A tool for identification of genes expressed in patterns of interest using the Allen Brain Atlas. *Bioinformatics*. 2009;**25**(13):1647–1654.
11. Girard F, *et al*. Gene expression analysis in the parvalbumin-immunoreactive PV1 nucleus of the mouse lateral hypothalamus. *Eur J Neurosci*. 2011;**34**(12):1934–1943.
12. Ng L, *et al*. An anatomic gene expression atlas of the adult mouse brain. *Nat Neurosci*. 2009;**12**(3):356–362.
13. Bilella A, *et al*. The Foxb1-expressing neurons of the ventrolateral hypothalamic parvafox nucleus project to defensive circuits. *J Comp Neurol*. 2016;**524**(15):2955–2981.
14. Mendelson WB, *et al*. The flower pot technique of rapid eye movement (REM) sleep deprivation. *Pharmacol Biochem Behav*. 1974;**2**(4):553–556.
15. Arthaud S, *et al*. Paradoxical (REM) sleep deprivation in mice using the small-platforms-over-water method: polysomnographic analyses and melanin-concentrating hormone and hypocretin/orexin neuronal activation before, during and after deprivation. *J Sleep Res*. 2015;**24**(3):309–319.
16. Maloney KJ, *et al*. c-Fos expression in dopaminergic and GABAergic neurons of the ventral mesencephalic tegmentum after paradoxical sleep deprivation and recovery. *Eur J Neurosci*. 2002;**15**(4):774–778.
17. Celio MR. Calbindin D-28k and parvalbumin in the rat nervous system. *Neuroscience*. 1990;**35**(2):375–475.

18. Ahnaou A, *et al*. Long-term enhancement of REM sleep by the pituitary adenylyl cyclase-activating polypeptide (PACAP) in the pontine reticular formation of the rat. *Eur J Neurosci*. 1999;**11**(11):4051–4058.
19. Fang J, *et al*. Pituitary adenylate cyclase activating polypeptide enhances rapid eye movement sleep in rats. *Brain Res*. 1995;**686**(1):23–28.
20. Palchykova S, *et al*. Manipulation of adenosine kinase affects sleep regulation in mice. *J Neurosci*. 2010;**30**(39):13157–13165.
21. Tatsuki F, *et al*. Involvement of Ca(2+)-dependent hyperpolarization in sleep duration in mammals. *Neuron*. 2016;**90**(1):70–85.
22. Pellegrini C, *et al*. Suppression of sleep spindle rhythmogenesis in mice with deletion of CaV3.2 and CaV3.3 T-type Ca(2+) channels. *Sleep*. 2016;**39**(4):875–885.
23. Anderson MP, *et al*. Thalamic Cav3.1 T-type Ca2+ channel plays a crucial role in stabilizing sleep. *Proc Natl Acad Sci U S A*. 2005;**102**(5):1743–1748.
24. Keating GL, *et al*. Wake promoting effects of cocaine and amphetamine-regulated transcript (CART). *Neuropeptides*. 2010;**44**(3):241–246.
25. Cvetkovic V, *et al*. Characterization of subpopulations of neurons producing melanin-concentrating hormone in the rat ventral diencephalon. *J Neurochem*. 2004;**91**(4):911–919.
26. Hanriot L, *et al*. Characterization of the melanin-concentrating hormone neurons activated during paradoxical sleep hypersomnia in rats. *J Comp Neurol*. 2007;**505**(2):147–157.
27. Chung S, *et al*. Identification of preoptic sleep neurons using retrograde labelling and gene profiling. *Nature*. 2017;**545**(7655):477–481.
28. Zhang Z, *et al*. An excitatory circuit in the perioculomotor midbrain for non-REM sleep control. *Cell*. 2019;**177**(5):1293–1307.e16.
29. Goutagny R, *et al*. Paradoxical sleep in mice lacking M3 and M2/M4 muscarinic receptors. *Neuropsychobiology*. 2005;**52**(3):140–146.
30. Brunner JI, *et al*. Pharmacological validation of candidate causal sleep genes identified in an N2 cross. *J Neurogenet*. 2011;**25**(4):167–181.
31. Niwa Y, *et al*. Muscarinic acetylcholine receptors Chrm1 and Chrm3 are essential for REM sleep. *Cell Rep*. 2018;**24**(9):2231–2247.e7.
32. Silvani A, *et al*. Multiple sleep alterations in mice lacking cannabinoid type 1 receptors. *PLoS One*. 2014;**9**(2):e89432.
33. Pava MJ, *et al*. Endocannabinoid signaling regulates sleep stability. *PLoS One*. 2016;**11**(3):e0152473.
34. Thomas AM, *et al*. Cntnap2 knockout rats and mice exhibit epileptiform activity and abnormal sleep/wake physiology. *Sleep*. 2017;**40**(1). doi:10.1093/sleep/zsw026
35. Kimura M, *et al*. Conditional corticotropin-releasing hormone overexpression in the mouse forebrain enhances rapid eye movement sleep. *Mol Psychiatry*. 2010;**15**(2):154–165.
36. Monti JM. Serotonin control of sleep-wake behavior. *Sleep Med Rev*. 2011;**15**(4):269–281.
37. Vyazovskiy VV, *et al*. Sleep EEG in mice that are deficient in the potassium channel subunit K.v.3.2. *Brain Res*. 2002;**947**(2):204–211.
38. Espinosa F, *et al*. Ablation of Kv3.1 and Kv3.3 potassium channels disrupts thalamocortical oscillations in vitro and in vivo. *J Neurosci*. 2008;**28**(21):5570–5581.
39. Datta S, *et al*. Endogenous and exogenous nitric oxide in the pedunculopontine tegmentum induces sleep. *Synapse*. 1997;**27**(1):69–78.
40. Pasumarthi RK, *et al*. Further characterization of sleep-active neuronal nitric oxide synthase neurons in the mouse brain. *Neuroscience*. 2010;**169**(1):149–157.
41. Morairty SR, *et al*. A role for cortical nNOS/NK1 neurons in coupling homeostatic sleep drive to EEG slow wave activity. *Proc Natl Acad Sci U S A*. 2013;**110**(50):20272–20277.
42. Jego S, *et al*. Tuberal hypothalamic neurons secreting the satiety molecule Nesfatin-1 are critically involved in paradoxical (REM) sleep homeostasis. *PLoS One*. 2012;**7**(12):e52525.
43. Vas S, *et al*. Nesfatin-1/NUCB2 as a potential new element of sleep regulation in rats. *PLoS One*. 2013;**8**(4):e59809.
44. Xu M, *et al*. Basal forebrain circuit for sleep-wake control. *Nat Neurosci*. 2015;**18**(11):1641–1647.
45. McDowell KA, *et al*. Sleep dysfunction and EEG alterations in mice overexpressing alpha-synuclein. *J Parkinsons Dis*. 2014;**4**(3):531–539.
46. Howell MJ, *et al*. Rapid eye movement sleep behavior disorder and neurodegenerative disease. *JAMA Neurol*. 2015;**72**(6):707–712.
47. Verret L, *et al*. Cholinergic and noncholinergic brainstem neurons expressing Fos after paradoxical (REM) sleep deprivation and recovery. *Eur J Neurosci*. 2005;**21**(9):2488–2504.
48. Verret L, *et al*. Localization of the neurons active during paradoxical (REM) sleep and projecting to the locus coeruleus moradrenergic neurons in the rat. *J Comp Neurol*. 2006;**495**:573–586.
49. Clément O, *et al*. The inhibition of the dorsal paragigantocellular reticular nucleus induces waking and the activation of all adrenergic and noradrenergic neurons : a combined pharamacological and functional neuroanatomical study. *PLoS One*. 2014;**9**(5):e96851.
50. Oh-I S, *et al*. Identification of nesfatin-1 as a satiety molecule in the hypothalamus. *Nature*. 2006;**443**(7112):709–712.
51. Foo KS, *et al*. Distribution and neuropeptide coexistence of nucleobindin-2 mRNA/nesfatin-like immunoreactivity in the rat CNS. *Neuroscience*. 2008;**156**(3):563–579.
52. Dominguez G, *et al*. Cart peptides: modulators of mesolimbic dopamine, feeding and stress. *Ann N Y Acad Sci*. 2004;**1025**:363–369.
53. Stanek LM. Cocaine- and amphetamine related transcript (CART) and anxiety. *Peptides*. 2006;**27**(8):2005–2011.
54. Koylu EO, *et al*. Cocaine- and amphetamine-regulated transcript peptide immunohistochemical localization in the rat brain. *J Comp Neurol*. 1998;**391**(1):115–132.
55. Abrahám H, *et al*. Ontogeny of cocaine- and amphetamine-regulated transcript (CART) peptide and calbindin immunoreactivity in granule cells of the dentate gyrus in the rat. *Int J Dev Neurosci*. 2007;**25**(5):265–274.
56. Brailoiu GC, *et al*. Nesfatin-1: distribution and interaction with a G protein-coupled receptor in the rat brain. *Endocrinology*. 2007;**148**(10):5088–5094.
57. Pałasz A, *et al*. Nesfatin-1, a unique regulatory neuropeptide of the brain. *Neuropeptides*. 2012;**46**(3):105–112.